Microfluid Nanofluid (2008) 5:529–540
DOI 10.1007/s10404-008-0265-9

RESEARCH PAPER

# Experimental study of diffusion-based extraction from a cell suspension

**Clara Mata · Ellen K. Longmire · David H. McKenna · Katie K. Glass · Allison Hubel**

Received: 30 August 2007 / Accepted: 29 January 2008 / Published online: 21 February 2008


**Abstract** A recently proposed application of microfluidics is the post-thaw processing of biological cells. Numerical simulations suggest that diffusion-based extraction of the cryoprotective agent dimethyl sulfoxide (DMSO) from blood cells is viable and more efficient than centrifugation, the conventional method of DMSO removal. In order to validate the theoretical model used in these simulations, a prototype was built and the flow of two parallel streams, a suspension of Jurkat cells containing DMSO and a wash stream that contained neither cells nor DMSO, was characterized experimentally. DMSO transport in a rectangular channel (depth 500 μm, width 25 mm and overall length 125 mm) was studied as a function of three dimensionless parameters: depth ratio of the streams, cell volume fraction in the cell solution, and the Peclet number (*Pe*) based on channel depth, average flow rate and the diffusion coefficient for DMSO in water. In our studies, values of *Pe* ranged from O($10^3$) to O($10^4$). Laminar flow was ensured by keeping the Reynolds number between O(1) and O(10). Experimental results based on visual and quantitative data demonstrate conclusively that a microfluidic device can effectively remove DMSO from liquid and cell laden streams without compromising cell recovery. Also, flow conditions in the microfluidic device appear to have no adverse effect on cell viability at the outlet. Further, the results demonstrate that we can predict the amount of DMSO removed from a given device with the theoretical model mentioned previously.

**Keywords** Diffusion · DMSO-extraction · Cell suspension · Microfluidics · Channel flow

C. Mata · E. K. Longmire
Department of Aerospace Engineering and Mechanics, University of Minnesota, Minneapolis, MN, USA

D. H. McKenna
Department of Laboratory Medicine and Pathology, University of Minnesota, Minneapolis, MN, USA

K. K. Glass · A. Hubel (✉)
Department of Mechanical Engineering, University of Minnesota, 1100 Mechanical Engineering, 111 Church St. S.E, Minneapolis, MN 55455, USA
e-mail: hubel001@umn.edu
URL: www.me.umn.edu/labs/lab3134

## 1 Introduction

Hematopoietic stem cells (HSC) have become the standard of care for a wide range of hematologic and non-hematologic diseases. Most protocols specify that hematopoietic stem cell products from bone marrow or peripheral blood are cryopreserved until the patient is ready to receive the transplant (Rowley 1992). Nearly all hematopoietic stem cell transplants from umbilical cord blood are performed using cryopreserved cells. Surveys by Areman et al. (1990a, b) showed that most clinical transplantation centers use a cryopreservation solution containing 10% v/v dimethyl sulfoxide (DMSO). The infusion of hematopoietic stem cells cryopreserved with DMSO into humans has been associated with adverse events (Alessandrino et al. 1999; Davis et al. 1990; Stroncek et al. 1991; Zambelli 1998). Studies of hematopoietic stem cell transplants by Zambelli et al. (1998), Martino et al. (1996), Smith et al. (1987), Iacone et al. (1991) and Syme et al. (2004) noted that the greater the dose of DMSO, the more severe the adverse reaction or that removing DMSO reduced the incidence and severity of the transfusion reaction. Antonenas et al. (2002) observed that removing the DMSO using conventional centrifugation results in a 95% removal and an

elimination of the adverse effects resulting from unwashed products.

Current strategies for removal of DMSO involve washing of cells upon thaw using a dextran/albumin solution and centrifuge-based technology. These approaches result in substantial cell loss. Antonenas et al. (2002) observed a loss of 27–30% of nucleated cells due to post-thaw washing of umbilical cord blood. Perotti et al. (2004) observed a similar loss. Laroche et al. (2005) suggested that the wash step be omitted particularly in certain categories of patients where the loss of cells may have a detrimental effect. Fleming and Hubel (2006) suggested that the development of methods to remove DMSO while minimizing cell losses would benefit all recipients of cryopreserved hematopoietic stem cell transplants. Ding et al. (2007) discuss the development of a new method of DMSO removal from cryopreserved blood cells. They suggest that large amounts of cells could be washed using hollow fibers, in which DMSO is transported across fiber membranes and cell membranes due to pressure and concentration gradients. However, no experimental results have been published yet. In the current work, we investigate a method using microfluidics to remove DMSO while minimizing cell losses.

The use of microfluidics to manipulate populations of cells has been addressed in several studies. Kumar et al. (2005) demonstrated the ability to separate cells based on size using acoustic and flow fields. Hawkes et al. (2004) employed sound waves to move cells from one buffer to another. At flow rates of 2.5 ml/min and very low cell concentrations (0.01% by volume), 70% of cells could be moved between the streams. Yang et al. (2005) used the Zweifach-Fung effect in a microfluidic device to bleed off a percentage of blood plasma from a suspension containing erythrocytes. Sethu et al. (2006a, b) used a microfluidic sieve to separate erythrocytes from leukocytes. These studies demonstrate the potential of microfluidics as a platform for cell processing. However, none of these techniques on its own appears viable for our application (to process clinical scale volumes of cells). In addition, these studies focused principally on the motion of cells and did not quantify or optimize the transport of chemical species in the surrounding liquids.

A common strategy in microfluidic liquid systems is to employ either pressure gradients or electric fields to initiate and control fluid motion, and thus, avoid moving structural parts that may damage cells. The motion is generally laminar, implying that fluid elements move along parallel streamlines and mix in the cross-stream direction by molecular diffusion only. As explained by Beebe et al. (2002), molecular diffusion across a distance $l$ is related to the diffusion time scale $\tau$ by $l^2 \sim D\tau$, where $D$ is the molecular diffusivity. Therefore when the distance $l$ is small, substantial cross-stream diffusion can occur during the flow passage through a microfluidic device. Various investigators (Brody and Yager 1997; Hatch et al. 2001; Weigl and Yager 1999) have demonstrated separation and immunoassay devices based on this principle, taking advantage of differences in molecular diffusion rates (molecular diffusivity) for different molecular sizes. Typically the diffusivity scales inversely with molecular or particle size so that, as opposed to liquid molecules ($\sim$nm), blood cells ($\sim$10 μm) do not diffuse significantly across streamlines in microfluidic devices. For example, the diffusivity of DMSO in water is $\sim 10^{-5}$ cm$^2$/s, while the same constant for a blood cell in water is $10^{-10}$ cm$^2$/s so that diffusion times of cells would be $10^5$ times longer than those of DMSO molecules (Bird et al. 2002).

In our problem, however, we do need to consider diffusion of DMSO across cell membranes. DMSO is present in both the intracellular and extracellular solutions and can move easily across the cell membrane (McGrath et al. 1988) by passive diffusion driven by differences in chemical potential. Thus, the extraction of DMSO from a cell suspension requires diffusion through cell membranes (intracellular) as well as across the flow stream (extracellular). Numerical simulations by Fleming et al. (2007) suggest that diffusion-based extraction of DMSO from blood cells in a microfluidic device is viable and efficient. The objective of this paper is to demonstrate DMSO extraction experimentally and, specifically, to demonstrate the possibility of processing clinical volumes of cell suspensions in short periods of time using microfluidic devices.

The following two sections describe the theoretical model developed by Fleming et al. (2007) against which the experimental results will be compared, the flow facility and experimental methods. Experimental results are presented and discussed in Sect. 4 of this paper. Concluding remarks follow in Sect. 5.

## 2 Theoretical model

The dimensions of our DMSO-removal device were chosen based upon the theoretical model by Fleming et al. (2007) outlined here. Two streams flow in parallel through a rectangular channel of constant cross sectional area (Fig. 1). The lower stream consists of a cryopreserved cell suspension, and the upper stream is a wash stream that contains neither cells nor DMSO. In the figure, $\delta$ and $d$ denote the depths of the lower stream and the channel, respectively. In general, DMSO diffuses from the cell stream to the wash stream. The coordinates $x$, $y$, and $z$ (not shown) are aligned with the streamwise, cross-stream, and spanwise directions.

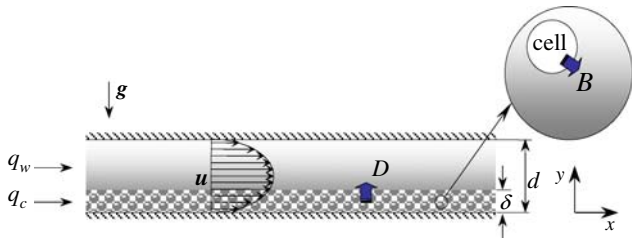


**Fig. 1** Schematic of the flow configuration. Two streams enter at *left* and flow in parallel toward the *right*. The lower stream contains a DMSO-laden cell suspension. The upper stream is a wash solution that does not contain DMSO. Exploded view illustrates the diffusion of DMSO from the intracellular to the extracellular space

A list of the assumptions considered by Fleming et al. (2007) and the system of equations they solved using a forward-marching finite difference algorithm follow:

- The flow is laminar, steady, two-dimensional and fully developed so that the streamwise velocity $u_x$ is a function of the depth alone.
- The viscosity is uniform across the entire depth so that the initial (and ongoing) velocity profile is parabolic.
- In the cell stream, the cells move with the local fluid velocity, and the possibility of cells settling due to gravity is ignored.
- The diffusion of DMSO from the intracellular solution to the extracellular solution in the cell stream was considered as a source or production of extracellular concentration.
- Variations across the depth are much stronger than the variations along the stream ($\partial^2/\partial x^2 << \partial^2/\partial y^2$).

The equation for transport of DMSO in the wash stream is:

$$u_x \frac{\partial C_t}{\partial x} = D \frac{\partial^2 C_t}{\partial y^2}, \tag{1}$$

where $D$ is the diffusion coefficient of DMSO and $C_t$ denotes the number of moles of DMSO per unit volume. The equations for transport of DMSO in the cell-laden stream are:

$$\frac{\partial C_t}{\partial x} = \frac{D}{u_x}\frac{\partial^2 C_t}{\partial y^2} + \frac{V_i B}{V_t u_x}(C_i - C_e) \tag{2}$$

and

$$\frac{\partial C_i}{\partial x} = \frac{B}{u_x}(C_e - C_i), \tag{3}$$

where the concentration $C_e$ is the number of moles of extracellular DMSO per local extracellular volume $V_e$, $C_i$ is the number of moles of intracellular DMSO per intracellular volume $V_i$, and $B$ is the membrane permeability to DMSO. For the cell stream, $C_t$ now represents the number of moles of extracellular DMSO in the local volume $V_t = V_i + V_e$ and $V_i/V_t$ is the local volume fraction of cells.

By scaling the streamwise velocity $u_x$ using the mean velocity within the channel $U$, and the coordinates $x$ and $y$ using the channel depth $d$, Eq. (2) becomes

$$\frac{\partial C_t}{\partial x^*} = \frac{1}{u^* Pe}\frac{\partial^2 C_t}{\partial y^{*2}} + \frac{V_i}{V_t} B^*(C_i - C_e), \tag{4}$$

where $x^*$ and $y^*$ are dimensionless coordinates and $u^*$ is a dimensionless streamwise velocity. In addition to $V_i/V_t$, also known as CVF (cell volume fraction) or cytocrit, two dimensionless parameters arise:

$$Pe = \frac{dU}{D} \quad \text{and} \quad B^* = \frac{Bd}{U}$$

$Pe$ is the Peclet number and $B^*$ can be considered as a reciprocal Peclet number related to cell membrane permeability. Another independent parameter is $\delta/d$. This depth ratio is directly related to the inlet flow rate fraction $f_q$, defined as:

$$f_q = \frac{q_c}{q_t},$$

where $q_t = q_c + q_w$ is the total volumetric flow rate through the channel. Here, $q_c$ and $q_w$ are the cell stream and wash stream flow rates, respectively. The flow rate fraction $f_q$ is related to $\delta/d$ through the parabolic variation of the velocity profile across the channel depth. Notice that the mean velocity $U$ may be expressed in terms of $q_t$ and the channel cross-sectional area $A$ as:

$$U = \frac{q_t}{A}.$$

A parameter to keep in mind is the Reynolds number, $Re$. For this system, the channel Reynolds number is defined as:

$$Re = \frac{\rho U d}{\mu},$$

where $\rho$ and $\mu$ are fluid density and viscosity, respectively. In all of the cases we examine, the Reynolds number is well below values characteristic of transitional or turbulent flows. The model described above is a direct function of the four dimensionless parameters $\delta/d$, $Pe$, $B^*$ and $V_i/V_t$. Exploration into the influence of these parameters on model performance can be found in the article by Fleming et al. (2007).

Dependent dimensionless variables of interest are the normalized average concentrations of outlet cell-laden and wash streams, respectively, defined as:

$$C_c^* = \frac{C_c}{C_0} \quad \text{and} \quad C_w^* = \frac{C_w}{C_0}.$$

## 3 Flow facility and experimental methods

### 3.1 Flow device

Our DMSO-removal device was fabricated following design criteria that are in agreement with the theoretical model already proposed. All experiments within this paper correspond to $Re < 12$ for which the flow is laminar, and the entry length is very short. Furthermore, we include adapters with constant cross sectional area to smooth the flow transitions from the inlet ports to the channel and from the channel to the outlet ports.

A single stage prototype (Fig. 2a) was fabricated and used to validate the model for DMSO extraction with and without cells, and also to visualize cell motion. The key component of this prototype is the DMSO-removal device which contains a single rectangular channel (Fig. 2b). The top, bottom and side walls are made of borosilicate glass (from microscope slides) to permit optimal visualization of flow from two orientations. All walls were glued together with a clear two-part epoxy. Constant cross sectional area adapters were glued to each end of the channel with the same type of epoxy. Each adapter consists of two identical pieces of Plexiglas® machined with a computer numerical control (CNC) mill that are held together with stainless steel screws and sealed with the same epoxy. A glass microscope coverslip cut to size was mounted inside the adapter at the entrance end of the channel to act as a divider or splitter. Nylon fittings (not shown in Fig. 2b) are used at inlet and outlet ports, located on top and bottom of each adapter and sealed with Buna-n gaskets. Dimensions and a detailed description of the flow through the device follow.

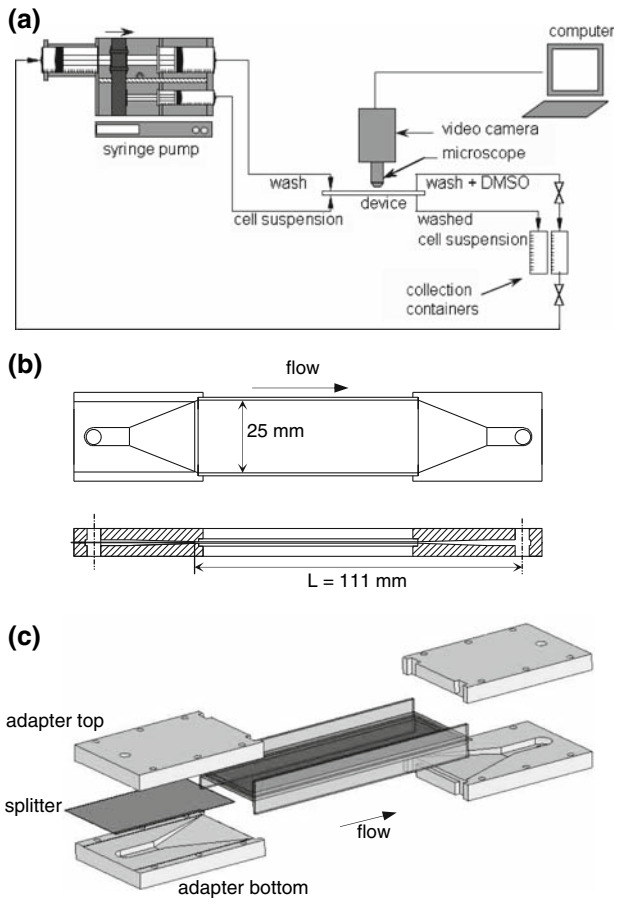


**Fig. 2** **a** Sketch of experimental set up. **b** Sketch of device (to scale), and **c** exploded view of the device (to scale)

Two streams enter the device through opposing ports (1.56 mm diameter) separated by the splitter plate. The splitter plate prevents mixing between the initially opposing streams and helps redirect the streams so that they flow in parallel. One of the adapters, which has a constant area cross section of 12.5 mm$^2$ and 25 mm length, feeds both streams into the rectangular channel of $d = 500$ μm depth, 25 mm width, and 75 mm length (the splitter plate terminates at the downstream end of this adapter). Downstream of this section, the other constant area adapter is used to transition flow from the channel to the round outlet ports (1.56 mm diameter). The overall length, from the tip of the splitter to the outlet ports, is $L = 111$ mm.

Once steady flow conditions were achieved, samples of both streams were collected downstream of the exit; the wash stream sample was collected in-line, in a Tygon® tube with a volumetric capacity of 5 ml, and the cell-laden stream sample was collected in a vial.

A Photron Fastcam-Ultima 512 high-speed digital video camera attached to a Leitz® Laborlux D microscope was used to visualize the flow through the prototype. The only source of light was a Schott ACE I Fiberoptic Illuminator. Videos were recorded on a desktop computer. The microscope was rotated to obtain both top and side views. Long working distance objectives were used to ensure visualization from top to bottom and from one side wall to a region near the channel's center. Details on flow control and stream characterization follow.

### 3.2 Flow rate control and measurement

A syringe pump (Harvard Apparatus, Inc. Model 22) drives the cell-laden and wash solutions contained in two separate syringes simultaneously into the device (see Fig. 2). The desired flow rate (±0.1 ml/min) for the wash solution is set in a controller attached to the pump; this makes the piston driving both syringes move at a certain speed. The volumetric ratio at which both solutions are driven is then equal to the ratio of the cross sectional area of the syringes. To ensure that the volumetric ratio at which cell-laden and wash streams are separated at the outlet ports is the same ratio at which they entered the device, a third syringe draws the wash stream leaving the device at the same rate this

solution is being driven-in. This is accomplished by attaching the third syringe to the back of the piston driving the other two syringes. Also, the cross sectional area of the syringes driving and drawing the wash stream must be the same. The cell-laden stream outlet is open to the atmosphere.

### 3.3 Stream characterization

A full characterization includes DMSO concentration, cell recovery and cell concentration. Procedures follow.

#### *3.3.1 DMSO concentration*

The concentration of DMSO in the streams was determined by spectrophotometry. The optical density (absorbance) of the solution at a wavelength of 209 nm was measured (SpectraMax$^{TM}$ Plus$^{384}$, Molecular Devices). The relationship between absorbance and concentration was determined through a two-step calibration process.

First, serial dilutions (0.1–$10^{-6}$ M) of a DMSO-laden solution were performed, and the absorbance as a function of concentration was quantified (Fig. 3a). The relationship between concentration and absorbance is linear over a limited range of value ($1 \times 10^{-4}$ to $2 \times 10^{-4}$). In the linear region, the absorbance varies between 1.000 and 2.000 O.D. (optical density).

Second, calibration curves were obtained for every new batch of DMSO-laden ($C_0 = 0.1$ M) and wash (0.0 M) solutions. Two sets of 5 ml samples of known normalized concentration $C^* = C/C_0$ were prepared by mixing samples of these DMSO-laden and wash solutions at different volume ratios. One set for $C^*$ between 0.10 and 0.30 (typical values of $C_w^*$) and the other set for $C^*$ between 0.30 and 0.60 (typical values of $C_c^*$). Samples of each set of solutions were serially diluted (four times), until the absorbance of the sample was in the linear range ($\sim$1.0000–2.000 O.D.). Example curves are shown in Fig. 3b, c.

The concentration of each outlet stream from the microfluidic device was quantified by serially diluting (four times) the collected sample and matching the absorbance reading to a normalized concentration, using curves such as those shown in Fig. 3b, c. DMSO concentrations of cell-laden samples were measured after discarding the cells by centrifugation.

DMSO concentration in both streams was measured for 48 different flow conditions; 31 of those correspond to experiments without cells and 17 to experiments with cells. For each flow condition, nine absorbance measurements were performed on each of the two samples (cell-laden and wash streams). The results were statistically analyzed.

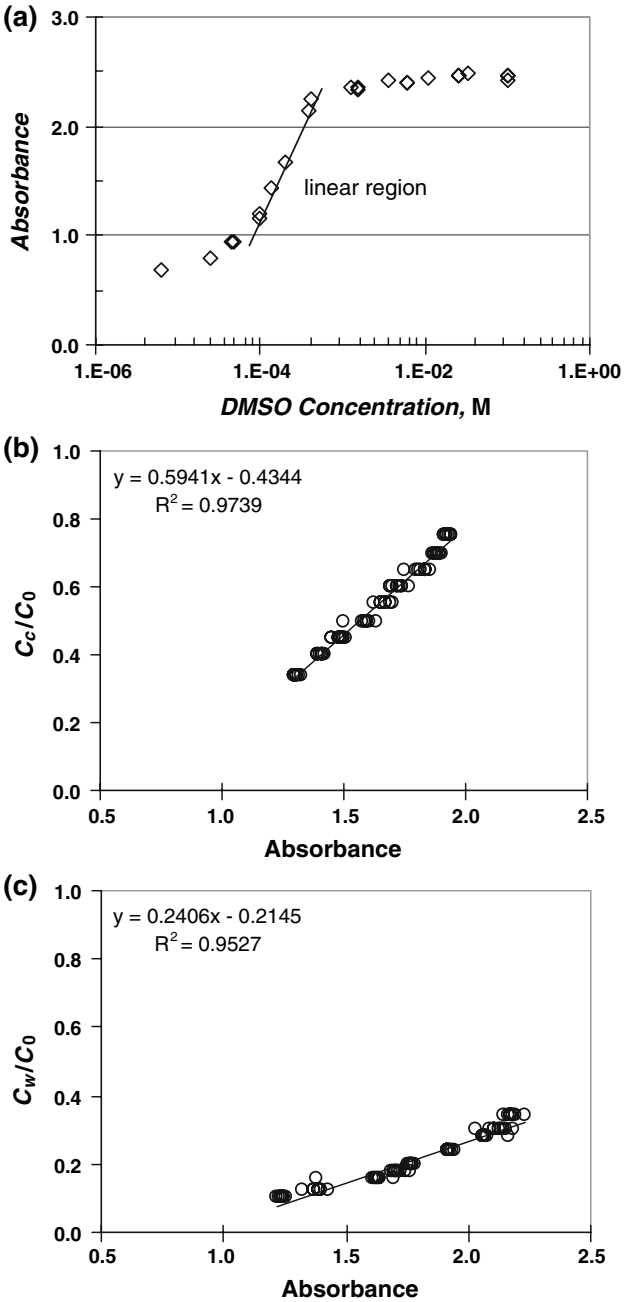


**Fig. 3** **a** Absorbance as a function DMSO molar concentration (typical curve). Only the linear region is considered useful to make measurements. **b**, **c** Examples of calibration curves for normalized DMSO concentration of cell and wash stream, respectively. $C_0 = 0.10$ v/v

Multiple linear and non-linear regressions were used to identify significant predictors for $C_c^*$ and $1 - C_w^*$, such as $f_q$ and $(1/Pe)^*(L/d)$. $P$ values less than 0.05 (statistically significant) were obtained. Mean values of normalized DMSO concentrations $C_c^*$ and $1 - C_w^*$ were calculated and plotted. Standard errors are reported in the plot legends.

### 3.3.2 Cell viability and cell recovery

Cell recovery from the device was determined using a hematocytometer (Hausser Scientific) combined with a membrane integrity dye. Briefly, a sample of cell suspension was recovered from the device outlet and stained for membrane integrity using acridine orange and propidium iodine. Cells that fluoresce green have intact membranes, and cells that fluoresce orange are dead. For a given sample, the total number of cells counted was greater than 200. Viability, the fraction of cells that are viable, is defined as the number of cells that fluoresce green divided by the total number of fluorescing cells. Cell Recovery is defined as the number of viable cells flowing out of the device divided by the number of viable cells flowing into the device. That is

$$\text{Recovery} = \frac{\text{Viability}_{\text{out}} \times \text{CVF}_{\text{out}}}{\text{Viability}_{\text{in}} \times \text{CVF}_{\text{in}}},$$

where $\text{CVF}_{\text{out}}$ denotes the cell volume fraction at the outlet and $\text{CVF}_{\text{in}}$ the cell volume fraction at the inlet (2%). This measure accounts for cells that may have died in the device. In addition to viability and recovery, the ratio $\text{CVF}_{\text{out}}/\text{CVF}_{\text{in}}$, which accounts for all cells, live and dead, was determined. This ratio quantifies the number of cells that may have accumulated in the channel during a test.

Six flow conditions were evaluated. Each flow condition was tested three times. Each time, three independent counts were performed for a total of 18 counts per flow condition: 9 at the inlet and 9 at the outlet. Then the data were statistically analyzed. Mean values of viability, cell concentration and recovery were calculated. The results are expressed as the mean ± SD (standard deviation). Multiple linear regressions were used to identify significant predictors for viability, concentration and recovery, such as, again, $f_q$ and $(1/Pe)^*(L/d)$. $P$ values less than 0.05 (statistically significant) were obtained. Cell counts were performed on both the wash and cell streams.

## 4 Results and discussion

### 4.1 Extraction of DMSO from a liquid stream

To characterize the extraction of DMSO in the device, studies were performed using a wash stream consisting of Phosphate Buffered Saline solution (PBS) and a DMSO-laden stream (PBS + 10% DMSO). Both streams were fed into the device at constant flow rates, and the DMSO concentration was determined for each outlet stream as a function of flow conditions. The range of total flow rate $q_t$ tested was 1.1–14.0 ml/min. The maximum flow rate of DMSO-laden stream tested was 8.2 ml/min.

The normalized DMSO-laden stream concentration $C_c^* = C_c/C_0$ as a function of $(1/Pe)^*(L/d)$, parameterized by the flow rate fraction $f_q$, is shown in Fig. 4a. Data were plotted against $(1/Pe)^*(L/d)$ because, as noted by Fleming et al. (2007), for a constant value of the Peclet number $Pe$, concentration data at different locations along the channel $x/d$ collapse to a single curve. This is especially convenient for scale up purposes when the channel aspect ratio $L/d$ becomes a variable of interest. It can be seen that $C_c^*$ rapidly decreases with $(1/Pe)^*(L/d)$ for $f_q$ constant, meaning that $C_c^*$ increases when the mean velocity $U$ increases [all the other variables in the parameter $(1/Pe)^*(L/d)$ are held constant]. The faster the flow, the smaller the number of moles of DMSO diffused from one stream to the other. Figure 4a also shows that $C_c^*$ increases when $f_q$ increases. Although the mean velocity $U$ is constant, when the flow rate fraction $f_q$ increases, the stream depth fraction $\delta/d$ also increases. Because the number of moles of DMSO to be transferred is larger and the volume of wash available to receive them is smaller, $C_c^*$ remains higher. Our experimental results demonstrate that the scale up of diffusion-based extraction of DMSO (or any other chemical compound) is more complex than suggested by Brody and Yager (1997), because it depends not only on the Reynolds number $Re$ (through the mean velocity $U$ and channel geometry), but also on parameters such as $(1/Pe)^*(L/d)$ and $f_q$.

The experimental values of $C_c^*$ are also compared with the model predictions for the same operating conditions and channel geometry, and the results match very well given the experimental uncertainty (Fig. 4a).

Measurements of the normalized wash stream concentration $C_w^* = C_w/C_0$ parameterized by the flow rate fraction $f_q$ are shown in Fig. 4b. These measurements are also plotted to further demonstrate the reliability of the concentration measurements, and the ability of the theoretical model to predict the outlet concentration. For convenience, the results are plotted as $1 - C_w^*$ versus $(1/Pe)^*(L/d)$. The quantity $1 - C_w^*$ shows the amount of DMSO moles leaving the lower stream, as opposed to the amount of DMSO moles entering the upper stream; this way the trends of the curves in Fig. 4a, b are similar. It can be seen that $1 - C_w^*$ rapidly decreases with $(1/Pe)^*(L/d)$ for $f_q$ constant, meaning as before that $C_w^*$ decreases when $U$ increases. Again, the faster the flow, the smaller the number of moles of DMSO diffused from one stream to the other. Figure 4b also shows that $1 - C_w^*$ decreases when $f_q$ increases, which is again consistent with the results in Fig. 4a. Finally, the experimental values of $1 - C_w^*$ are compared with the model predictions for the same operating conditions and channel geometry, and the results match very well given the experimental uncertainty, although a slight but systematic shift of the experimental points with respect to the theoretical curves is noticeable.

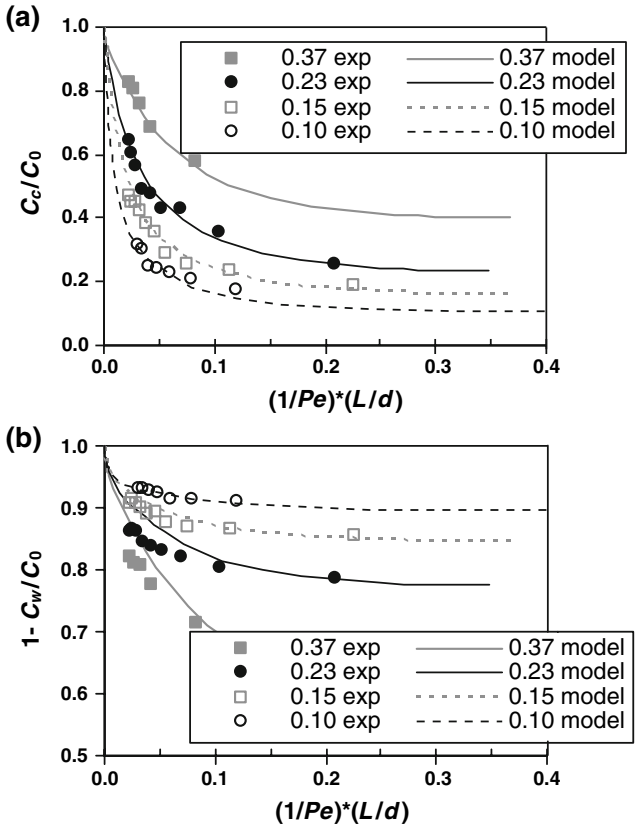


**Fig. 4** Extraction of DMSO from a liquid stream. **a** Normalized DMSO-laden stream concentration ($C_c/C_0$) as a function of $(1/Pe)^*(L/d)$ standard error = 4.16%. **b** Normalized concentration of DMSO in the outlet wash stream plotted as $1 - C_w/C_0$ as a function of $(1/Pe)^*(L/d)$ standard error = 1.53%. Experimental measurements are compared to the model predictions for the same flow conditions. Flow rate fractions $f_q$ of 0.1–0.37 were tested

The studies to date do not suggest a specific mechanism for the slight discrepancy between theory and experiment. However, we believe in two potential sources. First and most likely, DMSO is a highly polar molecule that interacts strongly with water. When the DMSO-laden stream encounters the wash stream, the interaction may cause a significant heat release, increasing the local temperature as well as the diffusion coefficient $D$ (Rosenbaum et al. 1971). A second possibility is that three-dimensionality generated by the channel geometry, i.e., presence of end walls, causes the discrepancy. However, numerical results using a three-dimensional laminar model rule out this possibility. Due to the high aspect ratio of our device, spanwise variations in velocity occurring near the end walls have negligible effect on the model predictions (i.e., the 3D model results match the 2D results presented to less than our uncertainty). In future studies, we will measure inlet and outlet temperatures to test the viability of this hypothesis and to possibly establish a mechanism for the discrepancy and therefore improve the model predictions.

### 4.2 Extraction of DMSO from a cell-laden stream

To demonstrate DMSO extraction from a cell-laden stream, several cases were examined using a lymphoblastic cell line (Jurkat cells, ATCC TIB-1522) to mimic a HSC product. The cell volumetric fraction CVF was 2%. The outlet concentration of DMSO in the wash stream and cell-laden stream supernatant (after centrifugation) was measured as a function of flow conditions for two flow rate fractions $f_q$. The experimental results are presented together with the corresponding model predictions in Fig. 5.

Figure 5a shows the normalized DMSO cell-laden stream concentration $C_c^*$ as a function of $(1/Pe)^*(L/d)$, for $f_q = 0.1$ and 0.23. The trends are identical to those observed in Fig. 4a, even though the transport of DMSO from the cell-laden stream to the wash stream occurs in two steps, from the cells to their surroundings (the cell-laden stream continuous phase) and then to the wash stream. Moreover, these results match the cell-laden model predictions given the experimental uncertainty.

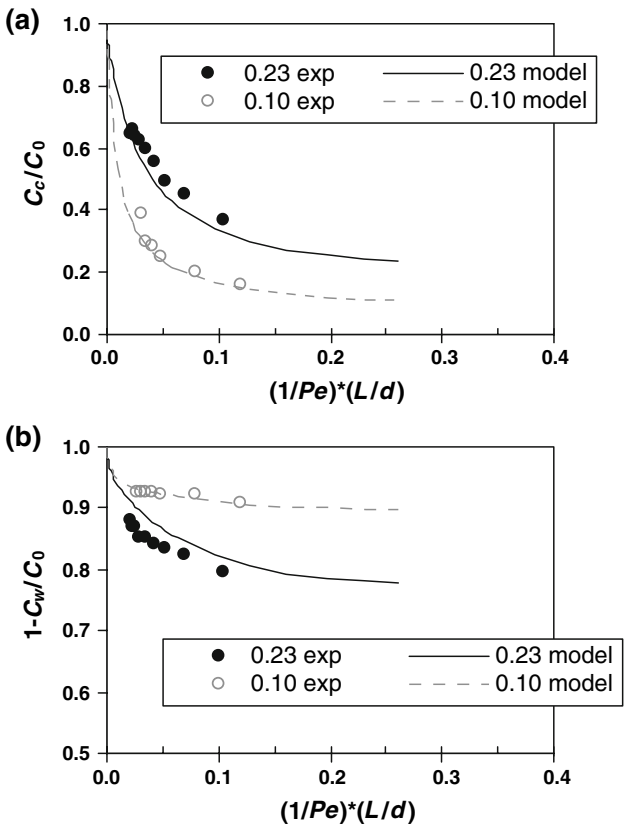


**Fig. 5** Extraction of DMSO from a cell-laden stream. **a** Normalized DMSO-laden stream concentration ($C_c/C_0$) as a function of $(1/Pe)^*(L/d)$ standard error = 2.74%. **b** Normalized concentration of DMSO in the outlet wash stream plotted as $1 - C_w/C_0$ as a function of $(1/Pe)^*(L/d)$ standard error = 1.31%. Experimental measurements (*circles*) are compared to the model predictions for the same flow conditions. Flow rate fractions $f_q$ of 0.1 and 0.23 were tested

Figure 5b shows the normalized wash stream concentration $C_w$* for $f_q = 0.10$ and 0.23, plotted as $1 - C_w$* versus $(1/Pe)$*$(L/d)$. The trends are identical to those observed in Fig. 4b.

In order to demonstrate the manner by which cells influence DMSO extraction from a DMSO-laden stream, the normalized concentration in the cell stream $C_c$* is replotted as a function of $(1/Pe)$*$(L/d)$ for cases with and without cells (Fig. 6). Besides the excellent agreement between experimental data and model predictions, it can be seen that at a given value of $(1/Pe)$*$(L/d)$, the DMSO concentration of the cell-laden stream is similar to the concentration of the DMSO-laden stream without cells. This result suggests that the presence of 2% cells in the DMSO-laden stream has no impact on the transport of DMSO from one stream to the other, as the theoretical model predicts. However, we expect that higher cytocrits will have an impact on the transport of DMSO from one stream to the other. As explained by Fleming et al. (2007), the difference in concentration reflects the DMSO contents inside of the cells; in the cell-laden stream, the amount of DMSO available for cross-stream diffusion, as seen by neighboring volume elements, is reduced compared to a stream without cells. In future studies, we will further investigate the effect of the cell volume fraction on the transport of DMSO.

### 4.3 Cell motion and recovery

In addition to removing DMSO, we are interested in minimizing cell losses. Therefore, additional studies were performed to observe cell motion and quantify cell recovery from the device. All cell motion studies described below were performed without modification of the channel surface to prevent cell adhesion. The cytocrit for these studies was 2%.

Still images of cells moving through the device are shown in Figs. 7 and 8. These images were extracted from the original high-resolution videos, after being downloaded from the high-speed digital camera to the computer. Unfortunately, the resolution is lost during the downloading and still image extraction process. When the two input streams (cell stream and wash stream) are flowed through the device, cells remain in the bottom section of the channel (Fig. 7). In all videos we have taken to date, flowing cells are visible as 'light' round spots with a darker border. In the still image (Fig. 7), individual cells are difficult to distinguish, but the cell-containing region appears darker than the wash region above it. The cells are uniformly distributed across the stream depth and do not appear to aggregate or migrate from the cell stream to the wash stream. Occasionally a few cells (<1%) appear to attach to the surface of the channel. However, visual examination of the channel did not indicate the presence of

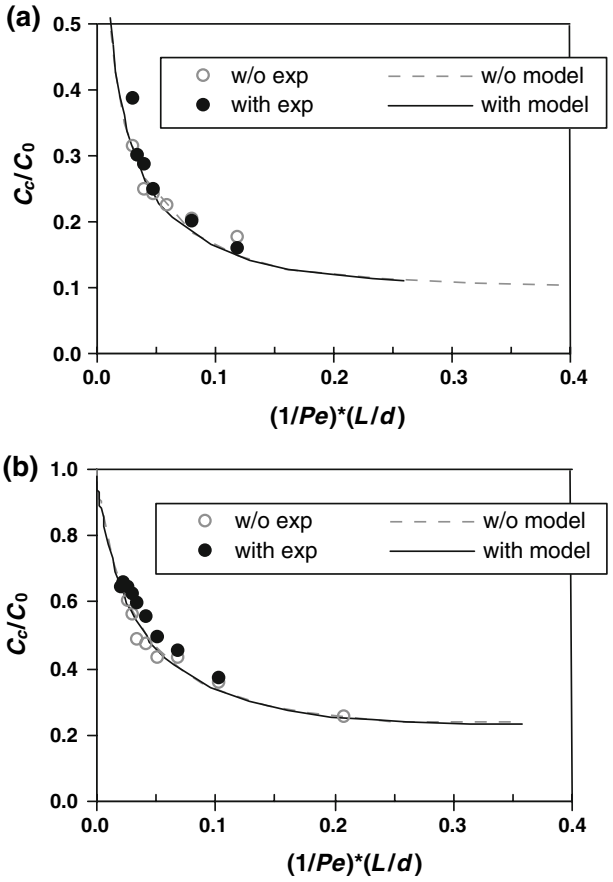


**Fig. 6** Normalized cell-laden stream concentration ($C_c/C_0$) as a function of $(1/Pe)$*$(L/d)$ for experimental measurements with 2% cells (*solid circles*) and without cells (*open circles*) and corresponding model predictions. **a** Flow rate fraction $f_q = 0.10$. **b** Flow rate fraction $f_q = 0.23$

significant numbers of cells remaining in the channel after completion of an experiment. To wash out dead cells that occasionally attach to the surface of the channel, the flow device was routinely flushed with phosphate buffered saline (PBS) and de-ionized (D.I.) water. The device has been flushed once per year with a 0.05% (v/v) Triton® X-100 solution, a non-ionic surfactant.

Visualization through the top of the channel revealed that cells were uniformly distributed across the span (Fig. 8). It also showed that cell motion was influenced by flow conditions. Under steady state conditions, the observed but not quantified cell volume fraction in the channel is larger than the nominal CVF of 2% (Fig. 8a, b). This does not mean that cells are accumulating in the channel, a non-steady state condition. It does indicate, however, that cells tend to pack more tightly for low cell stream flow rates $q_c$. In fact, the lower the value of $q_c$ the tighter the packing, at least for the conditions illustrated by Fig. 8 ($q_c = 0.28$, 0.85 and 1.41 ml/min, $f_q = 0.23$). Accumulation of cells in the channel was indeed observed

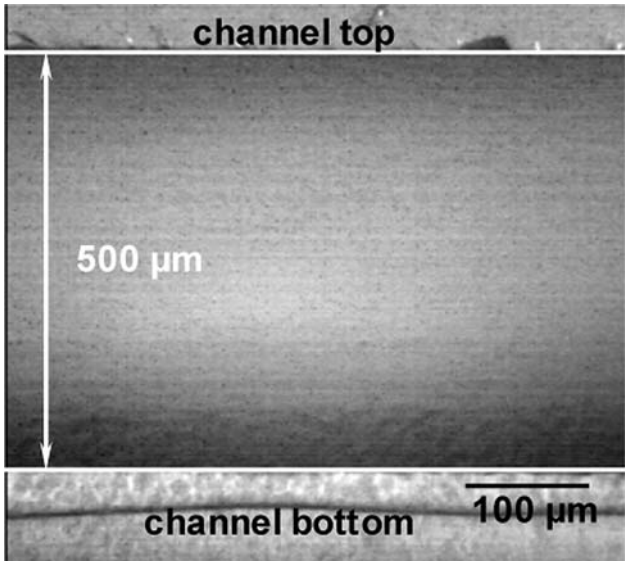


**Fig. 7** *Side view* Jurkat cell stream (*darker region* above channel bottom) flowing beneath wash stream with a flow rate fraction of $f_q = 0.23$. Image captured at mid region of the channel with a 10× objective. CVF = 2%, $Re = 0.9$, $Pe = 1{,}090$ and flow rate $q_c = 0.28$ ml/min

at low flow rates ($q_c < 0.28$ ml/min, $f_q = 0.10$). Any accumulation of cells could be cleared easily by increasing the mean flow rate indicating that the cells were not adhering to the channel. These results suggest that settling might become an issue at very low flow rates.

We were also interested in cell recovery from the device at practical volume fractions. Jurkat cells in a DMSO solution were flowed through the device and cell counts were performed at the inlet and outlet of the device to quantify cell recovery for a CVF of 2%. Three different flow rates were tested for each $f_q$. Cell counts were performed on samples from both wash and cell-laden streams. In general, no cells were observed in the wash stream samples, which always looked clear to the naked eye. Occasionally, a few cells (less than 10) were observed in the counting chamber while analyzing samples from the wash stream. We believe their presence in the chamber was due to improper cleaning of the chamber after previous measurements.

Results of cell recovery tests (cell-laden stream only) for flow rate fractions $f_q$ of 0.10 and 0.23 are shown in Table 1. In addition to viability and recovery, the ratio $CVF_{out}/CVF_{in}$, which accounts for all cells, live and dead, was determined. As we have mentioned, this ratio quantifies the number of cells that may have accumulated in the channel during a test.

The results reported in Table 1 are also plotted in Fig. 9. Figure 9a shows the viability at the inlet. Because the cell suspensions were freshly prepared, the viability was

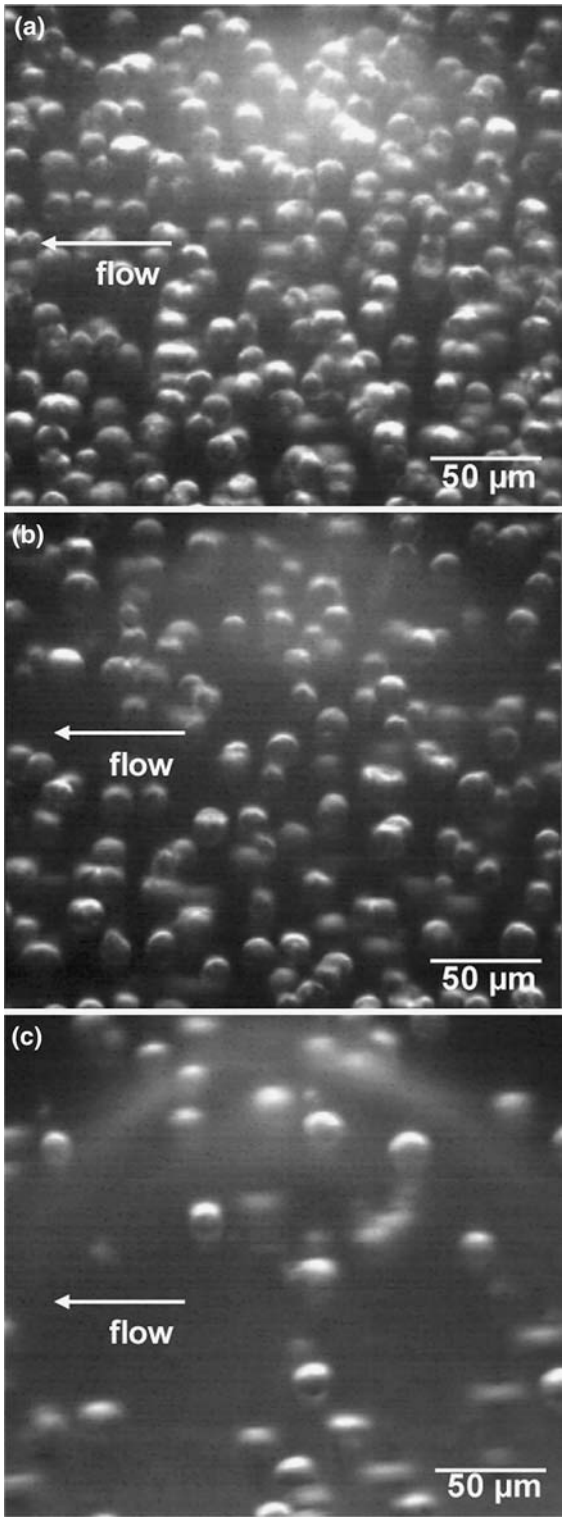


**Fig. 8** *Top view* Jurkat cell stream (CVF = 2%) flowing beneath wash stream with a flow rate fraction of $f_q = 0.23$. Images captured at mid region of the channel with a 20× objective. **a** $Re = 0.9$, $Pe = 1{,}090$ and flow rate $q_c = 0.28$ ml/min. **b** $Re = 2.6$, $Pe = 3{,}210$ and flow rate $q_c = 0.85$ ml/min. **c** $Re = 4.3$, $Pe = 5{,}340$ and flow rate $q_c = 1.41$ ml/min

**Table 1** Recovery of 2% v/v Jurkat cells in 10% DMSO suspension for various flow conditions in the device

| $f_q$ | $(1/Pe)^*(L/d)$ | $q_c$ (ml/min) | $\dot{\gamma}^a$ (1/s) | $\text{Viability}_{in}$ | $\text{Viability}_{out}$ | Recovery | $\text{CVF}_{out}/\text{CVF}_{in}$ |
|---|---|---|---|---|---|---|---|
| 0.10 | 8.0E-02 | 0.33 | 6.0 | 0.87 ± 0.02[b] | 0.92 ± 0.01 | 0.69 ± 0.03 | 0.66 ± 0.03 |
| | 4.8E-02 | 0.56 | 10.1 | 0.89 ± 0.00 | 0.93 ± 0.02 | 0.84 ± 0.03 | 0.81 ± 0.02 |
| | 3.4E-02 | 0.78 | 14.1 | 0.89 ± 0.02 | 0.94 ± 0.01 | 0.86 ± 0.06 | 0.82 ± 0.06 |
| 0.23 | 6.9E-02 | 0.85 | 6.4 | 0.89 ± 0.04 | 0.91 ± 0.01 | 0.97 ± 0.06 | 0.94 ± 0.07 |
| | 4.2E-02 | 1.41 | 10.6 | 0.89 ± 0.05 | 0.92 ± 0.01 | 0.93 ± 0.00 | 0.89 ± 0.04 |
| | 3.0E-02 | 1.98 | 14.8 | 0.88 ± 0.01 | 0.87 ± 0.01 | 0.98 ± 0.03 | 0.99 ± 0.03 |

[a] Local shear rate $\dot{\gamma} = u_c/\delta$

[b] Mean ± SD (standard deviation)

usually close to 0.90. In general, the viability at the outlet (Fig. 9b) was higher than the viability at the inlet, meaning that fewer dead cells were counted at the outlet. Because only whole cells fluoresce, it is possible that a fraction of the dead cells at the inlet somehow disintegrated while flowing through the device. Another possibility is that all of the dead cells at the inlet disintegrated while a few of the originally green fluorescent cells died within the device. Nevertheless, the flow conditions appear to have no significant adverse effect on the viability. As shown in Fig. 9c, cell recovery was very high for $f_q = 0.23$, it varied between 0.93 and 0.98. For $f_q = 0.10$, the recovery values were lower ($\leq$0.84). Because the number of intact cells flowing at any location is equal to the viability times the cell concentration, but the viability slightly increases after the cells flow through the device, this result suggests that a significant decrease in cell concentration must have occurred for $f_q = 0.10$, as actually shown in Fig. 9d. This is consistent with the cell accumulation in the device observed experimentally, particularly for the lowest flow rate tested for this flow rate fraction.

The exact cause of this accumulation remains unclear. We believe in two possible explanations, both related to gravitational settling overpowering lift due to flow convection. First and most likely, cells settle faster at lower flow rate fractions, because the stream depth fraction $\delta/d$ is lower, and the flow within the range $y < \delta$ is also on average slower. The instant the cell stream enters the device, cells begin settling due to gravity, and at the same total flow rate $q_t$, a greater percentage of cells will reach the bottom of the device for cell-laden streams of smaller depth $\delta$. As soon as the first cell touches bottom, trailing cells can encounter it, and accumulation can start. Also, accumulation will increase at low flow rates, because of the increase of the cells' residence time within the device. Although the experiments were run for similar mean velocities $U$ [that is, similar $(1/Pe)^*(L/d)$ as shown in Table 1], lower local velocities (lower $q_c$) are associated with $f_q = 0.10$ in comparison with $f_q = 0.23$. A second possible cause for the accumulation is that less lift will be generated when the

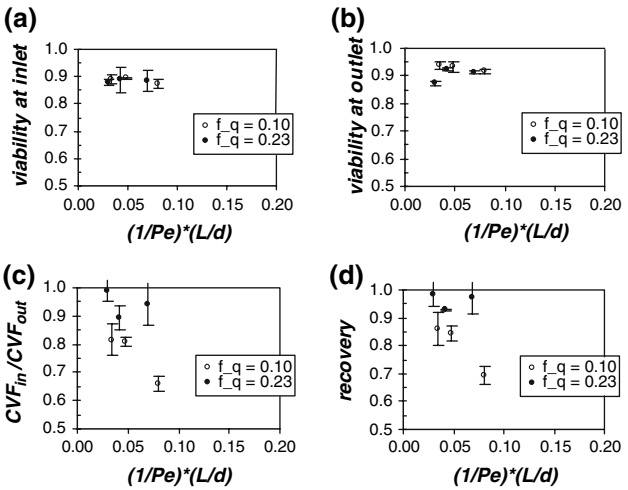


**Fig. 9** Results of cell recovery studies plotted as a function of $(1/Pe)^*(L/d)$, for $f_q = 0.1$ and 0.23. **a** Viability at the inlet. **b** Viability at the outlet. **c** Ratio of the cell volume fraction $\text{CVF}_{out}/\text{CVF}_{in}$. **d** Cell recovery

shear rate $\dot{\gamma}$ within the cell-laden stream is small. However, the local shear rate values shown in Table 1, calculated as local mean velocity ($u_c/\delta$) divided by the cell-laden stream depth $\delta$, rule out this possibility. It can be seen that similar shear rates $\dot{\gamma}$ yielded significantly different recovery values. In the future, we will continue our cell motion studies and also quantify cell recovery as a function of time to better understand the mechanisms of cell loss. Among these mechanisms, we expect to investigate possible osmotic damage to cells. Ding et al. (2007) considered cell volume change due to osmotic shock in their simulations of removal of DMSO from cryoprotective blood with hollow fiber modules. However, their simulations have not been compared with experimental data.

## 5 Concluding remarks

Our results demonstrate conclusively that a microfluidic device can be used to remove DMSO from liquid and cell

laden streams. Further, the results demonstrate that we can predict the amount of DMSO removed from a given device with the theoretical model described previously.

According to our results, flow conditions in a microfluidic device appear to have no adverse effect on the viability of cells. However, the results suggest that the cell-laden flow rate $q_c$ and flow rate fraction $f_q$ are important factors in cell recovery. Cell recovery was very high for $f_q = 0.23$, indicating the potential advantage of using a microfluidic device to remove DMSO from a cell-laden stream, as opposed to more conventional methods, such as centrifugation. We expect that larger flow rate fractions would also work well. Lower cell recovery was observed for $f_q = 0.10$, caused by cell accumulation in the device due to the low flow rates $q_c$ associated with this flow rate fraction. Nevertheless, as mentioned by Fleming et al. (2007), there is a practical lower limit for $f_q$ based on the need to process significant volumes of cell suspensions in a controllable and efficient manner. For example, clinical volumes of cell suspensions need to be processed in a reasonable amount of time (2–3 ml/min). Fleming et al. (2007) demonstrate how this could be done for specific parameter values. They pointed out that minimizing the flow rate fraction $f_q$, e.g., to values like 0.10, increases either the total width of the channel or the time required to process the desired volume. They conclude that DMSO removal may be accomplished more efficiently using multiple stages and larger $f_q$.

As discussed earlier, the source of the slight discrepancy between experimental results and theoretical predictions remains unclear. In future studies, we will continue our cell motion observations and also measure inlet and outlet temperatures in order to establish a mechanism for the discrepancy and therefore improve the model predictions. Additional work is also needed to determine the specific mechanism of cell loss at low volume fraction as well as optimal flow conditions for processing significant cell volumes with high recovery.

**Acknowledgments** This work was supported by the University of Minnesota Grant-in-aid Program, the National Blood Foundation and the National Institutes of Health (Grant No. R21EB004857). We would like to thank Brian Darr for his invaluable help and Dave Hultman, from the Research Shop at the Department of Electrical and Computer Engineering for helping with the design and fabrication of the microfluidic device. Anthony Cacace is acknowledged for helping with the exploded view of the channel.

## References

Alessandrino P et al (1999) Adverse events occurring during bone marrow or peripheral blood progenitor cell infusion: analysis of 126 cases. Bone Marrow Transplant 23(6):533–537

Antonenas V, Bradstock K, Shaw P (2002) Effect of washing proceedures on unrelated cord blood units for transplantation in children and adults. Cytotherapy 4(4):16

Areman EM, Sacher RA, Deeg HJ (1990a) Cryopreservation and storage of human bone marrow: a survey of current practices. Prog Clin Biol Res 333:523–529

Areman EM, Sacher RA, Deeg HJ (1990b) Processing and storage of human bone marrow: a survey of current practices in North America. Bone Marrow Transplant 6(3):203–209

Beebe DJ, Mensing GA, Walker GM (2002) Physics and applications of microfluidics in biology. Ann Rev Biomed Eng 4:261–286

Bird RB, Stewart WE, Lightfoot EN (2002) Transport phenomena. Wiley, New York

Brody J, Yager P (1997) Diffusion-based extraction in a microfabricated device. Sens Actuators A A58:13–18

Davis J, Rowley SD, Santos GW (1990) Toxicity of autologous bone marrow graft infusion. Prog Clin Biol Res 333:531–540

Ding W et al (2007) Simulation of removing permeable cryoprotective agents from cryopreserved blood with hollow fiber modules. J Membr Sci 288:85–93

Fleming KK, Hubel A (2006) Cryopreservation of hematopoietic and non-hematopoietic stem cells. Transfus Apher Sci 34:309–315

Fleming KK, Longmire EK, Hubel A (2007) Numerical characterization of diffusion-based extraction in cell-laden flow through a microfluidic channel. J Biomech Eng 129:703–711

Hatch A et al (2001) A rapid diffusion immunoassay in a T-sensor. Nat Biotechnol 19:461–465

Hawkes JJ et al (2004) Continuous cell washing and mixing driven by an ultrasound standing wave within a microfluidic channel. Lab Chip 4(5):446–452

Iacone A et al (1991) Density gradient separation of hematopoietic stem cells in autologous bone marrow transplantation. Haematologica 76(Suppl 1):18–21

Kumar M, Felke D, Belovick J (2005) Fractionation of cell mixtures using acoustic and laminar flow fields. Biotechnol Bioeng 89(2):129–137

Laroche V et al (2005) Cell loss and recovery in umbilical cord blood processing: a comparison of postthaw and postwash samples. Transfusion 45(12):1909–1916

Martino M et al (1996) Fractionated infusions of cryopreserved stem cells may prevent DMSO-induced major cardiac complications in graft recipients. Haematologica 81(1):59–61

McGrath JJ et al (1988) Low temperature biotechnology: emerging applications and engineering contributions. Presented at the winter annual meeting of the American Society of Mechanical Engineers, Chicago, IL, 27 November–2 December2, 1988. BED; **10**. The American Society of Mechanical Engineers, New York, vol viii, p 380

Perotti CG et al (2004) A new automated cell washer device for thawed cord blood units. Transfusion 44(6):900–906

Rosenbaum EE, Wood DC (eds) (1971) Dimethyl sulfoxide. Marcel Dikker Inc, New York

Rowley SD (1992) Hematopoietic stem cell processing and cryopreservation. J Clin Apher 7(3):132–134

Sethu P et al (2006a) Microfluidic isolation of leukocytes from whole blood for phenotype and gene expression analysis. Anal Chem 78(15):5453–5461

Sethu P, Sin A, Toner M (2006b) Microfluidic diffusive filter for apheresis (leukapheresis). Lab Chip 6(1):83–89

Smith DM et al (1987) Acute renal failure associated with autologous bone marrow transplantation. Bone Marrow Transplant 2(2):195–201

Stroncek DF et al (1991) Adverse reactions in patients transfused with cryopreserved marrow. Transfusion 31(6):521–526

Syme R et al (2004) The role of depletion of dimethyl sulfoxide before autografting: on hematologic recovery, side effects, and toxicity. Biol Blood Marrow Transplant 10(2):135–141

Weigl BH, Yager P (1999) Microfluidic diffusion-based separation and detection. Science 283:346–347

Yang S, Undar A, Zahn JD (2005) Blood plasma separation in microfluidic channels using flow rate control. Asaio J 51(5):585–590

Zambelli A et al (1998) Clinical toxicity of cryopreserved circulating progenitor cells infusion. Anticancer Res 18(6B):4705–4708